P-ISSN 2586-9000
E-ISSN 2586-9027
Homepage : https://tci-thaijo.org/index.php/SciTechAsia
Science & Technology Asia
Vol.27 No.1 January - March 2022
Page: [199-211]
Original research article

Magnetic Resonance Imaging (MRI) Lesion Patterns in Neuromyelitis Optica Spectrum Disorder (NMOSD)

Arvemas Watcharakorn[1,*], Supawan Sukpairoh[1], Varalee Mingkwansook[1], Puchit Sukphulloprat[2]

[1]*Department of Radiology, Faculty of Medicine, Thammasat University, Pathum Thani 12120, Thailand*
[2]*Department of Medicine, Faculty of Medicine, Thammasat University, Pathum Thani 12120, Thailand*

Received 6 July 2020; Received in revised form 14 December 2020
Accepted 15 January 2021; Available online 28 March 2022

ABSTRACT

We aimed to describe MRI lesion patterns in cases of NMOSD, aiding diagnosis of the disease. We retrospectively examined 27 patients with NMOSD, done by two neuroradiologists evaluating spinal cord, optic nerve and brain lesions. The mean number of involved spinal cord vertebral segments was 8.32 ±4.77 and the median longitudinal length was 11.4 centimeters (6.8-20.2). Spinal cord involvement ≥ 3 vertebral segments was found in 89.47% of patients. Concerning the location of spinal cord lesions, 84.21% were cervical, 57.9% were thoracic, and 57.9% were covered cervicomedullary junction. All spinal cord lesions showed both central and peripheral involvement on axial distribution and 94.74% of spinal cord lesions involved more than 50% of the cross-sectional area. Bright spotty lesions were found in 42.11% of patients. Bilateral optic neuritis was found in 83.33% of patients. These lesions involved more than half of the optic nerve length in 63.64% of patients. Brain MRI abnormalities were found in 88% of patients. The most frequently involved area was deep/subcortical white matter (76%). The second most frequently involved area was periependymal surface (60%).

MRI lesion patterns that are suggestive of NMOSD include longitudinal involvement of the spinal cord at three or more contiguous vertebral segments, both central and peripheral involvement on axial distribution which involves more than 50% as well as bilateral optic nerve involvement, and involvement in more than half of the optic nerve length. Cervical and cervicomedullary junction involvement seemed to be more common than thoracic involvement in Thai patients.

Keywords: Brain; Magnetic resonance imaging; MRI; Neuromyelitis optica spectrum disorder; NMOSD; Optic nerve; Spinal cord

***Corresponding author:** arvemas@yahoo.com
doi: 10.14456/scitechasia.2022.20

1. Introduction

Neuromyelitis optica (NMO) is a severe autoimmune inflammatory demyelinating disease of the central nervous system (CNS) [1]. NMO is clinically characterized by severe optic neuritis and transverse myelitis [2]. In the past, NMO was classified as a possible form of multiple sclerosis (MS) due to similarities in their clinical manifestations. Recently, NMO has become understood to be immunopathologically distinct from MS on the basis of clinical, pathological, and imaging features [1]. The role of autoimmunity in the etiopathogenesis of NMO was elucidated in 2004 after the discovery of aquaporin-4-immunoglobulin G (AQP4-IgG), an antibody against the astrocyte water channel [1]. The AQP4 channel is the most abundant water channel in the CNS; it is highly expressed in the optic nerve, spinal cord, periventricular areas, hypothalamus, and subpial regions, as well as in the brainstem and area postrema [1]. Moreover, neuromyelitis optica spectrum disorder (NMOSD) is a newly emerging disease spectrum with or without AQP4-IgG [2]. The demyelination process is not caused directly by AQP4-IgG, but is rather secondarily promoted by astrocytic injury [1]. Treatment strategies for attack prevention in NMOSD and MS differ [3]; moreover, some MS immunotherapies appear to aggravate NMOSD, indicating an imperative for early, accurate diagnosis [3].

Therefore, magnetic resonance imaging (MRI) has become an important tool for diagnosis of NMOSD, particularly for seronegative patients (AQP4-IgG negative) and for patients whose serologic AQP4-IgG status is unknown [1]. MRI has an increasingly important role in differentiating NMOSD from other inflammatory disorders of the CNS, particularly MS [4].

The prevalence of NMOSD in inflammatory demyelinating diseases of the CNS is much higher in Asia than in Western countries [5-6]. NMOSD is also more common than MS in Thai patients [7]. Most recent studies [8-13] on MRI findings in Asian populations were conducted on Japanese, Korean, and Chinese populations, only a few studies [14-15] were conducted on Thai populations. So, to fill this knowledge gap, we studied MRI lesion patterns in NMOSD cases, especially in Thai patients.

The aim of this study was to describe the MRI lesion patterns in NMOSD in Thai patients.

2. Materials and Methods

2.1 Patients

This retrospective study was approved by the Human Ethics Committee of our institution (Faculty of Medicine, Thammasat University). We retrospectively reviewed the medical records of patients with NMOSD at Thammasat University Hospital, Thailand, from January 2009 to August 2019. We included those who were 18 years or older and had fulfilled the 2015 International Panel for NMO Diagnosis (IPND) criteria [2]. Twenty-seven patients were included in our study. Patient demographic data were collected from the medical records. In AQP4 antibody seronegative patients, the clinical data were reviewed by a neurologist to confirm the diagnosis.

2.2 Image acquisition

MRI exams were performed using 1.5 Tesla scanners (Philips Achieva or Siemens Magnetom Aera) or 3 Tesla scanners (Siemens Magnetom Skyra). For patients who underwent MRI exams outside our hospital, images were also imported into our Picture Archiving and Communication System (PACS). These imported MRI data were obtained from a diverse array of hospitals using various MRI scanners. We evaluated the MRI studies that were obtained during clinical attack of NMOSD diagnosis at our hospital. Imaging data with motion artifacts that reduced diagnostic quality were excluded. Eligibility criteria were as follows: for spinal cord, both cervical and thoracic (including conus medullaris) axial and sagittal T2-

weighted images were analyzed; for optic nerve, orbital coronal and axial T2-weighted fat saturated (FS) or short tau inversion recovery (STIR) images were analyzed; for brain, axial T2-weighted and fluid attenuation inversion recovery (FLAIR) images were analyzed.

2.3 Image assessment

All images were evaluated independently by two neuroradiologists (8 and 10 years of experience in neuroimaging). Discrepancies in the assessment of morphologic features and characteristic signs were resolved by consensus. Values were averaged for the analysis.

For the spine, we counted the number of involved segments and measured the length of involvement (in centimeters) on sagittal T2-weighted images. We also evaluated cervicomedullary junction involvement. The cervicomedullary junction was defined as the area between a pontomedullary junction (as an upper border) and a line connecting the inferior aspect of C1 arch (as a lower border) on sagittal T2-weighted images. We identified the axial distribution into central lesions (which involved gray matter surrounding the central canal), peripheral lesions (which did not involve gray matter surrounding the central canal), and both central and peripheral lesions [10]. The axial extent of lesions was also assessed, as being either more or less than 50% of the spinal cord cross-sectional area. For morphological assessment and characteristic signs, we evaluated the presence of bright spotty lesions (defined as very hyperintense spotty lesions on axial T2-weighted images: the signal is visually more hyperintense than that of the surrounding cerebrospinal fluid without flow void effects [10]), spinal cord swelling, and spinal cord atrophy. If available, enhancement patterns were classified as patchy enhancement, ring enhancement pattern (a ring-like appearance of gadolinium enhancement surrounding a central zone of non-enhancement on axial T1-weighted postgadolinium sequences [16]), and lens-shaped appearance (a ring-like appearance of gadolinium enhancement surrounding a central zone of non-enhancement on sagittal T1-weighted postgadolinium sequences [16]).

For the orbits, we identified laterality and location (optic nerve, optic chiasm, and optic tract) of T2-hyperintense lesions on FS or STIR images. The extent of optic nerve involvement was also assessed, as being either more or less than half the nerve length. We evaluated the presence of optic nerve swelling, optic nerve atrophy, and optic nerve enhancement (if available T1-weighted postgadolinium images).

For the brain, we identified location of lesions on axial T2-weighted and FLAIR images (deep/subcortical white matter, white matter tract, basal ganglia, thalamus, hypothalamus, brainstem, cerebellum, and periependymal surface). We evaluated characteristic signs of arch bridge appearance (large, multifocal, edematous, and heterogeneous callosal lesions involving the full-thickness of the corpus callosum on axial T2-weighted and FLAIR images [17]) and marbled appearance (edematous and heterogeneous hyperintense callosal lesions on sagittal T2-weighted or FLAIR images [1,4], if available). We visually assessed the morphology of chronic lesions. If T1-weighted postgadolinium images were available, enhancement of lesions was assessed. Enhancement patterns were classified as cloud-like enhancement (patchy and inhomogeneous enhancement with poorly defined margins [1]), pencil-thin enhancement (thin linear enhancement along the surface of the ventricular system [1]) or flame-like appearance (when pencil-thin enhancement is associated with cloud-like enhancement [1]).

2.4 Statistical analyses

Continuous variables are expressed as mean ± SD for normal distributions or median (interquartile range) for non-normal distributions, while categorical variables are described as numbers and percentages.

3. Results

3.1 Demographics

Of the 27 Thai patients with NMOSD, 24 were female and 3 were male. The mean age at diagnosis was 49.11 ±12.95 years (range 25-73 years). Twenty-two patients (81.48%) were seropositive for AQP4 antibodies. The most frequent presenting symptoms were acute myelitis and optic neuritis, both about 70%. The median time interval between the symptoms to MRI study was 5 days (interquartile range, 1-21 days) for spinal MRI and 3.5 days (interquartile range, 1-12.5 days) for orbital MRI. Detailed patient demographics are summarized in Table 1.

3.2 Spinal cord analyses

Fourteen seropositive NMOSD patients and 5 seronegative NMOSD patients had spinal MRI eligible for review. As shown in Fig. 1, the peak of the location was high in the cervical spinal regions. Concerning the location of the spinal cord lesions, 84.21% (16/19) were in the cervical spinal cord, 57.9% (11/19) were in the thoracic spinal cord, and 57.9% (11/19) were covered cervicomedullary junction (Fig. 2a). The mean number of vertebral segments in cases of involved spinal cord was 8.32 ±4.77 (range 2-18), and the median longitudinal length was 11.4 centimeters (interquartile range, 6.8-20.2 centimeters). Spinal cord involvements of ≥3 vertebral segments (Fig. 2a) were found in 89.47% (17/19) of patients.

The spinal cord lesions in all patients showed both central and peripheral involvement on axial distribution and 94.74% (18/19) of spinal cord lesions involved more than 50% of the spinal cord cross-sectional area (Fig. 2b). Bright spotty lesions (Fig. 2c) were found in 42.11% (8/19) of patients. The incidence of spinal cord swelling (Fig. 2a) was 57.9% (11/19), while for spinal cord atrophy (Fig. 2d) it was 21.05% (4/19).

Table 1. Patient demographics (n=27)[a].

Demographics	NMOSD
Number of females	24/27 (88.89%)
Age at onset (mean ±SD) (years)	49.11 ±12.95
Ethnicity	
– Thai	27/27 (100%)
AQP4-IgG	
– Positive	22/27 (81.48%)
– Negative	5/27 (18.52%)
Presenting symptoms [b]	
– Optic neuritis	19/27 (70.37%)
– Acute myelitis	19/27 (70.37%)
– Area postrema syndrome	1/27 (3.70%)
– Acute brainstem syndrome	0/27 (0%)
– Symptomatic narcolepsy or acute diencephalic clinical syndrome	0/27 (0%)
– Symptomatic cerebral syndrome	1/27 (3.70)
Time interval between the symptoms to MRI study (median) (interquartile range) (days)	
– **Spinal MRI**	**5 (1-21)**
▪ 1-15 days	14/19 (73.68%)
▪ 16-30 days	4/19 (21.05%)
▪ 31-60 days	0/19 (0%)
▪ >60 days	1/19 (5.26%)
– **Orbital MRI**	**3.5 (1-12.5)**
▪ 1-15 days	10/12 (83.33%)
▪ 16-30 days	1/12 (8.33%)
▪ 31-60 days	0/12 (0%)
▪ >60 days	1/12 (8.33%)

[a] Data are number and percentage unless otherwise indicated.
[b] According to the core clinical characteristics of the 2015 IPND criteria.

Seventeen patients had post gadolinium injection MRI data available to review. Five patients had no enhancing lesion. Twelve of 17 patients (70.59%) exhibited a contrast enhancing area in which the most common pattern was patchy enhancement (Fig. 2e). Furthermore, 1 patient (5.88%) also exhibited a ring enhancement pattern (Fig. 2f) and 3 patients (17.65%) also exhibited a lens-shaped appearance (Fig. 2g). Detailed features of spinal MRI are shown in Table 2.

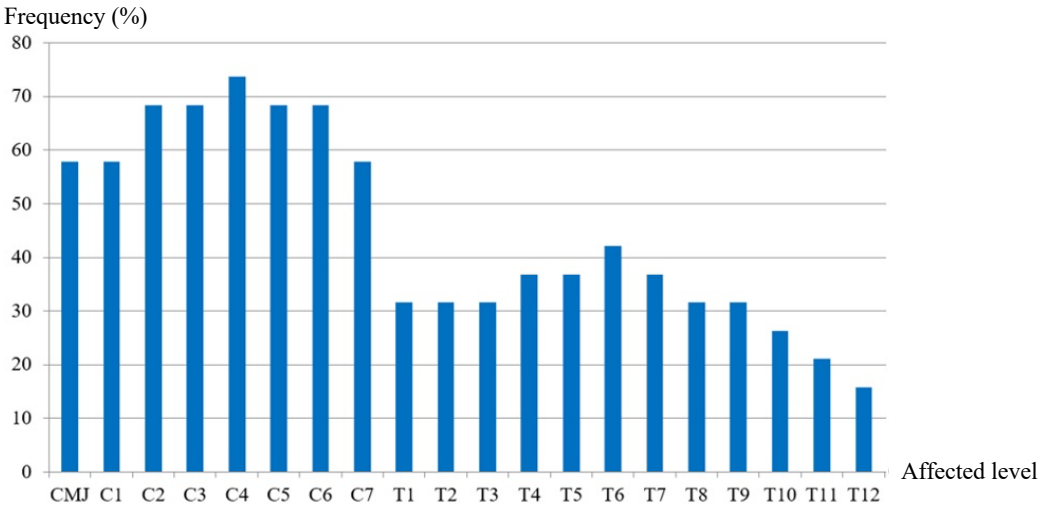

Cervicomedullary junction (CMJ)	Cervical vertebral segment 1-7 (C1-C7)	Thoracic vertebral segment 1-12 (T1-T12)
11/19 (57.90%)	16/19 (84.21%)	11/19 (57.90%)

Fig. 1. Frequency of affected levels of spinal cord lesions.

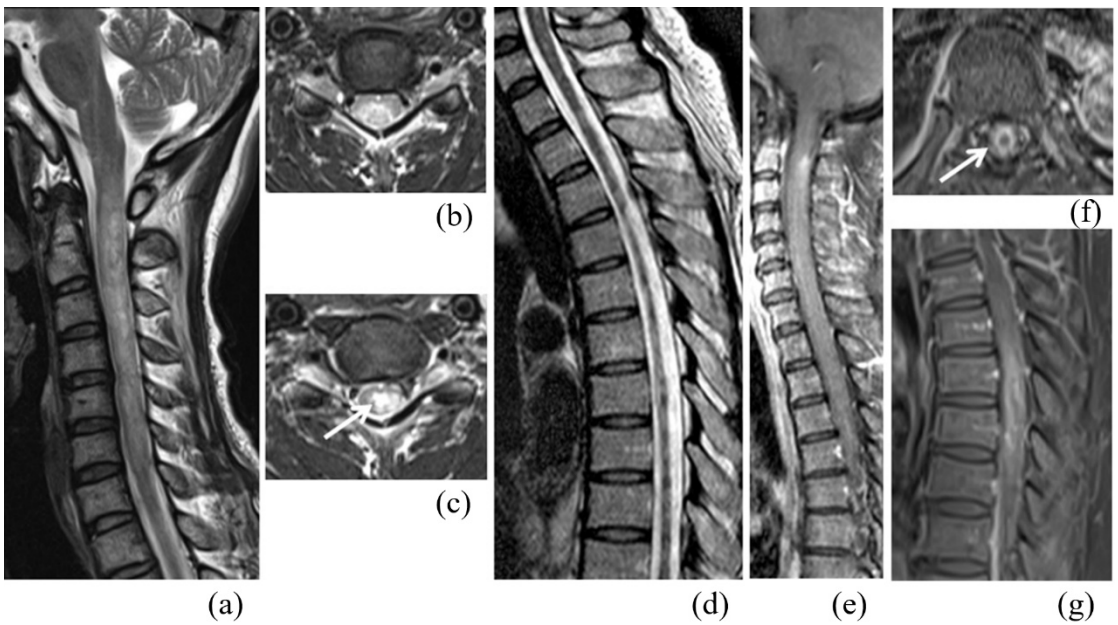

Fig. 2. Spinal cord involvement. (a) Sagittal T2-weighted image shows long spinal cord lesion more than 3 vertebral segments with cervicomedullary junction involvement and spinal cord swelling; (b, c) Axial T2-weighted images show both central and peripheral involvement and extent more than 50% of the spinal cord cross-sectional area (b) and a bright spotty lesion (c, arrow); (d) Sagittal T2-weighted image shows spinal cord atrophy; (e) Sagittal T1-weighted fat saturated postgadolinium image shows patchy enhancement; (f) Axial and (g) sagittal T1-weighted fat saturated postgadolinium images show a ring enhancement (f, arrow) and a lens-shaped enhancement (g).

Table 2. Spinal cord MRI findings (n=19)[a].

Imaging features	NMOSD
Location of lesions	
– Cervical	16/19 (84.21%)
– Thoracic	11/19 (57.90%)
– Cervicomedullary junction	11/19 (57.90%)
– Length of cord lesions (median) (interquartile range) (cm)	11.4 (6.8-20.2)
– Number of vertebral segments involved (mean ±SD)	8.32 ±4.77
– ≥3 vertebral segments	17/19 (89.47%)
Axial distribution	
– Central	0/19 (0%)
– Peripheral	0/19 (0%)
– Both	19/19 (100%)
Axial extent	
– > 50% of the cord area	18/19 (94.74%)
Morphology	
– Swelling	11/19 (57.90%)
– Atrophy	4/19 (21.05%)
Characteristic Sign	
– Bright spotty lesions	8/19 (42.11%)
Enhancement [b]	
– No enhancement	5/17 (29.41%)
– Enhancement	12/17 (70.59%)
▪ Patchy enhancement	12/17 (70.59%)
▪ Ring enhancement	1/17 (5.88%)
▪ Lens-shaped appearance	3/17 (17.65%)

[a] Data are number and percentage unless otherwise indicated.
[b] 17 of 19 patients had post gadolinium injection MRI available to review.

3.3 Optic nerve analyses

Ten seropositive NMOSD patients and 2 seronegative NMOSD patients had orbital MRI data eligible for review. Of these, 83.33% (10/12) had bilateral optic neuritis (Fig. 3a). Lesions that involved more than half of the optic nerve length (Fig. 3a) occurred in 63.64% (14/22) of these cases. Further, 58.33% (7/12) of these patients had optic chiasm (Fig. 3b,c) and optic tract involvement.

Incidence of optic nerve swelling was 31.82% (7/22), for optic nerve atrophy incidence was 9.09% (2/22).

All 12 patients had post gadolinium injection MRI data available to review. Ten patients (83.33%) exhibited contrast enhancement after gadolinium injection (Fig. 3d,e). Detailed features of orbital MRI are shown in Table 3.

Table 3. Optic nerve MRI findings (n=12)[a].

Imaging features	NMOSD
Laterality of lesions [b]	
– Unilateral	2/12 (16.67%)
– Bilateral	10/12 (83.33%)
Location of lesions	
– Optic nerve	
<1/2	8/22 (36.36%)
>1/2	14/22 (63.64%)
– Optic chiasm	7/12 (58.33%)
– Optic tract	7/12 (58.33%)
Morphology	
– Swelling	7/22 (31.82%)
– Atrophy	2/22 (9.09%)
Enhancement [c]	10/12 (83.33%)
– Optic nerve	15/22 (68.18%)
<1/2	7/22 (31.82%)
>1/2	8/22 (36.36%)
– Optic chiasm	4/12 (33.33%)
– Optic tract	2/12 (16.67%)

[a] Data are number and percentage unless otherwise indicated.
[b] Defined as laterality of optic nerve
[c] All patients had post gadolinium injection MRI available to review.

3.4 Brain analyses

Twenty seropositive NMOSD patients and 5 seronegative NMOSD patients had brain MRI data eligible for review. Twenty-two patients had brain lesions. The most frequently involved areas were deep or subcortical white matter (Fig. 4a), found in 76% (19/25) of patients. The second most frequently involved area was periependymal surface (Fig. 4b), found in 60% (15/25) of patients. Corpus callosal lesions were noted in 24% (6/25), basal ganglia lesions in 24% (6/25), thalamic lesions in 16% (4/25), hypothalamic lesions in 8% (2/25), and cerebellar lesions in 8% (2/25) of patients. Brainstem lesions were also detected in 24% (6/25) of patients; lesions were composed of pontine involvement in 3 patients and medullary involvement at the area of postrema (Fig. 4c,d) in 3 patients.

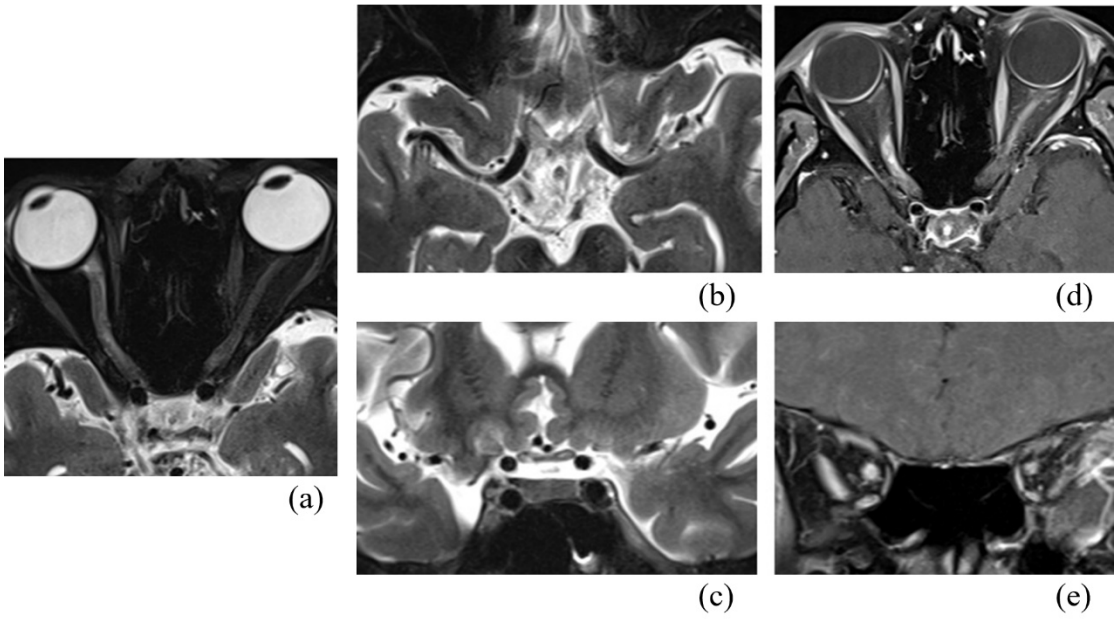

Fig. 3. Optic nerve involvement. (a) Axial T2-weighted fat saturated image shows bilateral optic nerve involvement which involved more than half of the optic nerve length; (b) Axial and (c) coronal T2-weighted fat saturated images show optic chiasm involvement; Axial (d) and coronal (e) T1-weighted fat saturated postgadolinium images show bilateral optic nerve enhancement.

There was no arch bridge appearance found in 6 patients with corpus callosal lesions. In addition, 56% (14/25) of the patients had sagittal T2-weighted or FLAIR images available to review and only 50% (3/6) of the patients with corpus callosal lesions (Fig. 4d) had sagittal T2-weighted or FLAIR images available. We found no marbled appearance of the corpus callosal lesions on the sagittal T2-weighted or FLAIR images in these 3 patients.

The frequency of chronic lesions in patients was 20% (5/25).

Twenty-four patients had post gadolinium injection MRI data available to review. Merely 3 of 24 (12.50%) patients had enhancing lesions. Specific contrast enhancement patterns were also analyzed. There were 1/24 (4.17%) patients with cloud-like enhancement and 3/24 (12.5%) patients with pencil-thin enhancement. Therefore, the one patient had both cloud-like and pencil-thin enhancements, so-called flame-like enhancement (Fig. 4e,f), 1/24 (4.17%). Detailed features of brain MRI data are shown in Table 4.

4. Discussion

In our study, we reported demographics data in Thai NMOSD patients. The age at onset of NMOSD in the patients in our study corresponds to other studies with female predilection [6, 8, 11]. Transverse myelitis and optic neuritis were the most common presenting symptoms in this study. The same has been reported in other studies [8,11] which found that transverse myelitis and optic neuritis were common in NMOSD patients. In this study, most patients (>90%) had a time interval between the appearance of symptoms and their MRI study of less than 1 month. Our study confirms the typical MRI lesion patterns in the spinal cord. Longitudinal involvement of the spinal cord at three or more contiguous vertebral segments is a characteristic spinal cord lesion of NMOSD [8, 11, 14].

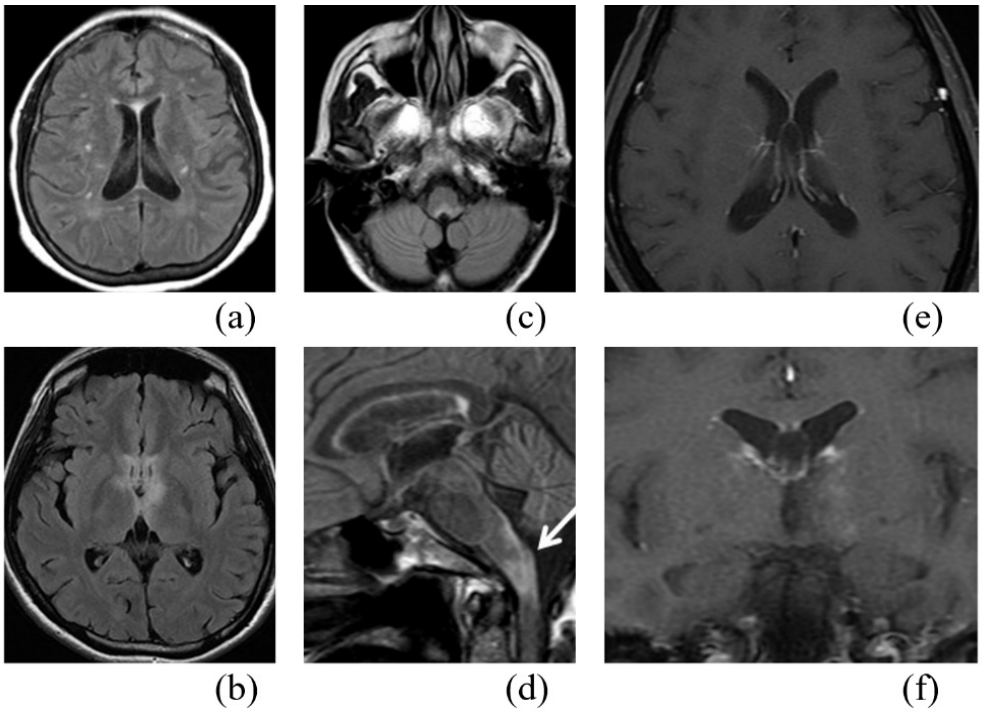

Fig. 4. Brain involvement. (a-c) Axial FLAIR images show lesions involving deep and subcortical white matter (a), periependymal surface of lateral and third ventricles (b) and area of postrema (c); (d) Sagittal FLAIR images show corpus callosal lesions and lesion involving area of postrema (arrow); Axial (e) and coronal (f) T1-weighted fat saturated postgadolinium images show pencil-thin enhancement (e, f) and cloud-like enhancement (f). Both cloud-like enhancement and pencil-thin enhancement, so called flame-like enhancement (f).

The NMOSD spinal cord lesions were more commonly located in the cervical and thoracic cord in previous studies [11, 18, 19]. Recently, Tatekawa et al. [8] reported a bimodal distribution of spinal cord lesions which had a high peak in the thoracic region (71%), more so than in the cervical region (29%). In our study, cervical cord involvement (84.21%) was found more frequently than thoracic cord involvement (57.90%). So, our results showed a difference in peaks as compared to the study of Tatekawa et al. [8]. However, the high peak in the cervical region in our study corresponds to the results of a few other prior studies [12, 20]. Furthermore, cervicomedullary involvement was more frequently found in our study (57.90%) which was quite higher than findings by Chee et al. [9]. A high peak of spinal cord lesions in the cervical region and frequent cervicomedullary junction involvement in this study are comparable to results of Tritrakarn et al. [14], which was done in the Thai population and also showed more common involvement of cervical/cervical to medulla regions than the thoracic region. We suggest that spinal cord lesions in the cervical region and cervicomedullary junction involvement can be diagnostic clues in imaging diagnosis of NMOSD in the proper clinical context, especially in Thai patients.

All spinal cord lesions in this study were located both central and peripheral distribution on axial images and most of them (94.74%) involved more than 50% of the cross-sectional cord area, similar to previous studies [9-11, 14]. Spinal cord swelling and atrophy were more frequent in NMOSD than in MS [8, 14]. Our study found that spinal

cord atrophy occurred in 21.05% of patients, which resembles findings from previous studies [8,14] (about 29.0-29.8%). In contrast, we found 57.90% of the patients had spinal cord swelling, a higher percentage than previous studies [8,14] (about 32.3-33.3%). Yonezu et al. [10] reported that bright spotty lesions are a finding specifically seen in NMOSD, occurring in 54% of the patients; the authors hypothesized that the bright spotty lesions might reflect microcystic changes (intense damage of the spinal cord). Alternatively, Zalewski et al. [16] suspected bright spotty lesions might be related to focal regions of increased edema or cerebrospinal fluid trapping. In our study, bright spotty lesions were also common, found in 42.11% of patients. We hypothesize that cavitation of the spinal cord results in brighter (fluid) T2 signal areas.

Table 4. Brain MRI findings (n=25)[a].

Imaging features	NMOSD
No lesion	3/25 (12%)
Location of lesions	
– Deep/subcortical white matter	19/25 (76%)
– White matter tract	
▪ Corpus callosum	6/25 (24%)
▪ Corticospinal tract	1/25 (4%)
– Basal ganglia	6/25 (24%)
– Thalamus	4/25 (16%)
– Hypothalamus	2/25 (8%)
– Brainstem	6/25 (24%)
▪ Midbrain	0/25 (0%)
▪ Pons	3/25 (12%)
▪ Medulla: Area of postrema	3/25 (12%)
– Cerebellum	2/25 (8%)
– Periependymal surface	15/25 (60%)
Morphology	
– Chronic lesions	5/25 (20%)
Characteristic Signs	
– Marbled appearance [b]	0/14 (0%)
– Arch bridge appearance	0/25 (0%)
Enhancement [c]	
– No enhancement	21/24 (87.5%)
– Enhancement	3/24 (12.5%)
▪ Cloud-like enhancement	1/24 (4.17%)
▪ Pencil-thin enhancement	3/24 (12.5%)
▪ Flame-like enhancement	1/24 (4.17%)

[a] Data are number and percentage unless otherwise indicated.
[b] 14 of 25 patients had sagittal T2-weighted or FLAIR images available to review.
[c] 24 of 25 patients had post gadolinium injection MRI available to review.

A contrast enhancing area of spinal cord lesion was detected in 70.59% of the MRI exams available to review. Similarly, Chee et al. [9] reported enhancing spinal cord lesions in 63.42% of cases. In our study, patchy enhancement was the most common enhancing pattern of spinal cord lesions, similar to findings of Chee et al. [9]. Zalewski et al. [16] also reported spinal cord ring-enhancing lesions occurring in 32% of cases that could be distinguished as NMOSD, ruling out other causes of longitudinally extensive myelopathy, but on its own did not distinguish NMOSD from MS. However, we found the ring enhancement pattern on axial imaging only in 5.88% of patients and the lens-shaped appearance on sagittal imaging in only 17.65% of patients. This difference might be due to different study populations, varying imaging protocol, and imaging quality. The pathophysiology of ring-enhancement of NMOSD is uncertain [16].

Our study showed that optic neuritis in NMOSD usually involved both optic nerves, similar to previous studies [15,21-23]. In particular, optic neuritis was strongly associated with longitudinally extensive involvement (more than half the optic nerve length), consistent with previous studies [21,22]. Our study also demonstrated frequent chiasmal and optic tract involvement, occurring at about 58.33%, equally, corresponding to previous studies [21-24].

We found optic nerve swelling and atrophy occurring in 31.82% and 9.09% of patients, respectively. Similarly, Tatekawa et al. [8] also reported optic nerve swelling and atrophy in NMOSD patients occurring in 23.8% and 11.9% of patients, respectively.

In this study, enhancing lesions of the optic nerve were detected in 68.18% of MRI exams available to review, corresponding to previous studies [22,23]. In contrast, Srikajon et al. [15] previously reported optic nerve enhancement in 26.1% of Thai patients. This difference might be due to the use of different MRI scanners, and a different proportion of enhancing images to review.

Brain involvement in NMOSD patients is more prevalent in Asian populations [13]. Brain lesions developed in 81% of NMOSD patients from Taiwan [25] and 64.7% of NMOSD patients from Korea [13]. Whereas studies in Caucasian populations reported lower prevalence of brain MRI abnormalities among NMOSD patients, about 25.6-41.6% [26-28]. Brain abnormalities in NMOSD might reflect high disease activity [13]. Our study found that 88% of NMOSD patients had brain MRI abnormalities during their clinical period, comparable to prior studies in Asian populations [13,25]. Our results might support the idea that Asian NMOSD patients have a more aggressive form of the disease. Actively demyelinating NMOSD lesions demonstrate vessel hyalinization.

In our study, lesions were most frequently shown in deep/subcortical white matter, about 76%. Kim et al. [13] reported juxtacortical/subcortical/deep white matter was most frequently involved, occurring in 58.8% of patients, comparable to our study. Periependymal regions are known to have high AQP4 expression and our study showed a rate of 60% periependymal involvement. Similar findings by Liao et al. [25] showed periventricular lesions in 60% of patients. Moreover, we found 24% (6/25) of patients had corpus callosal lesions. Similarly, Nakamura et al. [29] found 4 of 22 (18.2%) patients had callosal lesions. Among these 4 patients, 3 had marbled pattern corpus callosal lesions.

Among our 6 patients with corpus callosal lesions, only 3 had sagittal T2-weighted or FLAIR images available to review, and no marbled appearance in these 3 patients was found. This difference in results from Nakamura et al. [29] might be partly due to a lack of sagittal images. The mechanisms by which the corpus callosum is involved in NMOSD are unclear [29].

Kim et al. [13] reported cavity formation was detected in 29% of patients. Similarly, we also found chronic lesions in 20% of patients.

Three of twenty-four (12.5%) patients exhibited gadolinium contrast enhancement, comparable to previous studies [13,17], which reported the presence of brain lesion enhancement in 9-36% of patients. Although occurrence of cloud-like enhancement was reported at 29% in a study by Kim et al. [13], no patient in a study by Tatekawa et al. [8] showed this sign. We found only 4.17% of patients with cloud-like enhancement. Banker et al. [30] reported that pencil-thin ependymal enhancement may be a helpful radiological marker of NMOSD that can used to differentiate this condition from MS. They speculate that ependymal enhancement is due to an NMO-IgG-mediated autoimmune reaction against APQ4 water channels, which are heavily expressed in the ependymal region. Our study found 12.5% patients with pencil-thin enhancement. Systematic studies are needed to estimate frequencies of ependymal enhancement and periependymal abnormalities in patients with NMOSD [30].

This study had several limitations. First, there was a small number of patients who fulfilled the 2015 IPND criteria. This might be due to the low prevalence of NMOSD. Second, we were unable to compare differences between seropositive and seronegative NMOSD groups due to the low number of patients, especially the seronegative group. Third, there were different MRI scanners and imaging protocols used from various facilities because this study used a retrospective design. This might have influenced the detection and characterization of lesions in each part. To reduce the resulting variation, we used eligibility criteria for imaging analysis. Looking to the future, a prospective, multicenter study of NMOSD patients is planned.

5. Conclusion

We found typical MRI lesion patterns according to the 2015 IPND criteria in Thai patients. MRI lesion patterns that are suggestive of NMOSD include longitudinal involvement of the spinal cord at three or more contiguous vertebral segments, and both central and peripheral involvement on axial distribution which involves more than 50% of the cross-sectional area. Cervical and cervicomedullary junction involvement seemed to be more common than thoracic involvement in Thai patients. Bright spotty lesions (highly specific sign) were also common, found in 42.11% of our patients. Bilateral optic nerve involvement and involvement of more than half the optic nerve length are patterns strongly associated with NMOSD. The frequently involved areas of brain lesion patterns are deep/subcortical white matter and periependymal surface.

References

[1] Dutra BG, da Rocha AJ, Nunes RH, Maia ACM. Neuromyelitis optica spectrum disorders: Spectrum of MR imaging findings and their differential diagnosis. Radiographics 2018;38(1):169-93.

[2] Akaishi T, Nakashima I, Sato DK, Takahashi T, Fujihara K. Neuromyelitis optica spectrum disorders. Neuroimaging Clin N Am 2017;27(2):251-65.

[3] Wingerchuk DM, Banwell B, Bennett JL, Cabre P, Carroll W, Chitnis T et al. International consensus diagnostic criteria for neuromyelitis optica spectrum disorders. Neurology 2015;85(2):177-89.

[4] Kim HJ, Paul F, Lana-Peixoto MA, Tenembaum S, Asgari N, Palace J et al. MRI characteristics of neuromyelitis optica spectrum disorder: an international update. Neurology 2015;84(11):1165-73.

[5] Ochi H, Fujihara K. Demyelinating diseases in Asia. Curr Opin Neurol 2016;29:222-8.

[6] Vanikieti K, Poonyathalang A, Jindahra P, Bouzika P, Rizzo Iii JF, Cestari DM. Clinical characteristics and long-term visual outcome of optic neuritis in neuromyelitis optica spectrum disorder: A comparison between Thai and American-Caucasian cohorts. Mult Scler Relat Disord 2017 Oct;17:87-91.

[7] Apiwattanakul M, Kasemsuk C. NMO spectrum disorders comprise the major portion of CNS inflammatory diseases in Thai patients: a cross sectional study. Mult Scler Relat Disord 2014;3:61-6.

[8] Tatekawa H, Sakamoto S, Hori M, Kaichi Y, Kunimatsu A, Akazawa K et al. Imaging differences between neuromyelitis optica spectrum disorders and multiple sclerosis: a multi-institutional study in Japan. AJNR Am J Neuroradiol 2018;39:1239-47.

[9] Chee CG, Park KS, Lee JW, Ahn HW, Lee E, Kang Y et al. MRI features of aquaporin-4 antibody-positive longitudinally extensive transverse myelitis: insights into the diagnosis of neuromyelitis optica spectrum disorders. AJNR Am J Neuroradiol 2018;39:782-7.

[10] Yonezu T, Ito S, Mori M, Ogawa Y, Makino T, Uzawa A et al. “Bright spotty lesions” on spinal magnetic resonance imaging differentiate neuromyelitis optica from multiple sclerosis. Mult Scler 2014;20(3):331-7.

[11] Lin A, Zhu J, Yao X, Lin S, Murong S, Li Z. Clinical manifestations and spinal cord magnetic resonance imaging findings in Chinese neuromyelitis optica patients. Eur Neurol 2014;71(1–2):35-41.

[12] Zhang W, Jiao Y, Cui L, Liu L, Zhang L, Jiao J. Etiological, clinical, and radiological features of longitudinally extensive myelopathy in Chinese patients. J Clin Neurosci 2016;32:61-6.

[13] Kim JE, Kim SM, Ahn SW, Lim BC, Chae JH, Hong YH et al. Brain abnormalities in

neuromyelitis optica. J Neurol Sci 2011;302:43-8.

[14] Tritrakarn S, Jitprapaikulsan J, Thakolwiboon S, Piyapittayanan S, Ngamsombat C, Chawalparit O et al. Evaluation of the nmosd 2015 imaging guideline to differentiate between diagnosis of multiple sclerosis and neuromyelitis optica spectrum disorder in Thai patients. Neurology Asia 2018;23(1):61-8.

[15] Srikajon J, Siritho S, Ngamsombat C, Prayoonwiwat N, Chirapapaisan N. Differences in clinical features between optic neuritis in neuromyelitis optica spectrum disorders and in multiple sclerosis. Mult Scler J Exp Transl Clin 2018;4:1-12.

[16] Zalewski NL, Morris PP, Weinshenker BG, Lucchinetti CF, Guo Y, Pittock SJ et al. Ring-enhancing spinal cord lesions in neuromyelitis optica spectrum disorders. J Neurol Neurosurg Psychiatry 2017;88(3):218-25.

[17] Wang KY, Chetta J, Bains P, Balzer A, Lincoln J, Uribe T et al. Spectrum of MRI brain lesion patterns in neuromyelitis optica spectrum disorder: a pictorial review. Br J Radiol 2018;91(1086):1-8.

[18] Tackley G, Kuker W, Palace J. Magnetic resonance imaging in neuromyelitis optica. Mult Scler 2014;20:1153-64.

[19] Krampla W, Aboul-Enein F, Jecel J, Lang W, Fertl E, Hruby W et al. Spinal cord lesions in patients with neuromyelitis optica: a retrospective long-term MRI follow-up study. Eur Radiol 2009; 19: 2535-43.

[20] Kiyat-Atamer A, Ekizoglu E, Tuzun E, Kurtuncu M, Shugaiv E, Akman-Demir G et al. Long-term MRI findings in neuromyelitis optica: seropositive versus seronegative patients. Eur J Neurol 2013; 20:781-7.

[21] Mealy MA, Whetstone A, Orman G, Izbudak I, Calabresi PA, Levy M. Longitudinally extensive optic neuritis as an MRI biomarker distinguishes neuromyelitis optica from multiple sclerosis. J Neurol Sci 2015;355(1-2):59-63.

[22] Ramanathan S, Prelog K, Barnes EH, Tantsis EM, Reddel SW, Henderson AP et al. Radiological differentiation of optic neuritis with myelin oligodendrocyte glycoprotein antibodies, aquaporin-4 antibodies, and multiple sclerosis. Mult Scler 2016;22(4):470-82.

[23] Khanna S, Sharma A, Huecker J, Gordon M, Naismith RT, Van Stavern GP. Magnetic resonance imaging of optic neuritis in patients with neuromyelitis optica versus multiple sclerosis. J Neuroophthalmol 2012;32(3):216-20.

[24] Storoni M, Davagnanam I, Radon M, Siddiqui A, Plant GT. Distinguishing optic neuritis in neuromyelitis optica spectrum disease from multiple sclerosis: a novel magnetic resonance imaging scoring system. J Neuroophthalmol 2013;33:123-7.

[25] Liao MF, Chang KH, Lyu RK, Huang CC, Chang HS, Wu YR et al. Comparison between the cranial magnetic resonance imaging features of neuromyelitis optica spectrum disorder versus multiple sclerosis in Taiwanese patients. BMC Neurol 2014;14:1-9.

[26] O'Riordan JI, Gallagher HL, Thompson AJ, Howard RS, Kingsley DP, Thompson EJ, et al. Clinical, CSF, and MRI findings in Devic's neuromyelitis optica. J Neurol Neurosurg Psychiatry 1996;60:382-7.

[27] Ghezzi A, Bergamaschi R, Martinelli V, Trojano M, Tola MR, Merelli E, et al. Clinical characteristics, course and prognosis of relapsing Devic's Neuromyelitis Optica. J Neurol 2004;251:47-52.

[28] Collongues N, Marignier R, Zephir H, Papeix C, Blanc F, Ritleng C, et al. Neuromyelitis optica in France: a multicenter study of 125 patients. Neurology 2010;74:736-42.

[29] Nakamura M, Misu T, Fujihara K, Miyazawa I, Nakashima I, Takahashi T et al. Occurrence of acute large and edematous callosal lesions in neuromyelitis optica. Mult Scler 2009;15:695-700.

[30] Banker P, Sonni S, Kister I, Loh JP, Lui YW. Pencil-thin ependymal enhancement in neuromyelitis optica spectrum disorders. Mult Scler 2012; 18:1050–53.